


Nature of thermally excited vortical flow in a microsized nematic volume

A. V. Zakharov*

Saint Petersburg Institute for Machine Sciences, the Russian Academy of Sciences, Saint Petersburg 199178, Russia

P. V. Maslennikov†

Immanuel Kant Baltic Federal University, Kaliningrad 236040, Str. Universitetskaya 2, Russia (Received 10 September 2018; revised manuscript received 8 November 2018; published 11 March 2019)

The theoretical description of the reorientational dynamics in the case of a hybrid-oriented two-dimensional (2D) liquid crystal (LC) cell, under the influence of a temperature gradient ∇T , caused by a heat flux \mathbf{q} directed at an angle α across the lower bounding surface with the orientational defect, has been presented. Our calculations, based on the appropriate nonlinear extension of the classical Ericksen-Leslie theory, show that due to interaction between ∇T and the gradient of the director field $\nabla \mathbf{n}$ in the LC sample a thermally excited vortical fluid flow is maintained in the bulk of the nematic volume. In order to elucidate the role of both the orientational defect and the heat flux \mathbf{q} in formation of the vortical flow in the microsized LC volume, we have analyzed the response of the LC material confined in the microsized 2D volume on the effect of the laser beam focused on the bounding surface.

DOI: [10.1103/PhysRevE.99.032701](https://doi.org/10.1103/PhysRevE.99.032701)**I. INTRODUCTION**

The development of future biodynamics applications requires complicated investigations of natural and soft materials with multicoupling interactions of inner fields initiated by external forces. Decreasing of cell sizes down to nanolevel provides a close connect nematics model with biological liquid [1]. A challenging problem in all such applications is the precise handling of liquid microvolume, which requires self-contained micropumps of small package size exhibiting a very small displacement volume. Recently, the problem of motion of an ultra-thin (a few microliters) liquid crystal (LC) drop confined in the microsized volume between two horizontal and two lateral surfaces and subjected to uniform heating both from below and above, has been considered [2,3]. It has been shown that in the case of a hybrid-oriented two-dimensional (2D) LC cell, the direction and magnitude of the hydrodynamic flow \mathbf{v} produced by induced heating influences the director reorientation $\mathbf{n}(\mathbf{r}, t)$ across the LC cell. Understanding how the LC material deforms under the influence of the temperature gradient is a question of great fundamental interest, as well as an essential piece of knowledge in soft material science. Despite the fact that certain qualitative and quantitative advances in a hydrodynamic description of the relaxation processes in the LC phase under the influence of the temperature gradient have been achieved, it is still too early to talk about the development of a theory which would make it possible to describe the dissipation processes in confined LC phase with accounting for the orientational defects both in the bulk of the LC sample as well as on the bounding surfaces [4].

Note that a thin horizontal layer of quiescent LC fluid heated from below becomes unstable to convection via the Rayleigh-Benard mechanism, and this system has been used extensively for the study of a great variety of pattern-formation phenomena [5]. In that case the fluid is driven by maintaining the lower surface at a temperature ΔT above the upper surface temperature. The control parameter describes the instability, the Rayleigh number $R = \alpha g d^3 \Delta T / ((\alpha_4 / 2\rho_m) \kappa_\perp)$, where g is the gravitational acceleration, α is the isobaric thermal expansion coefficient, $\alpha_4 / 2\rho_m$ corresponds to the isotropic kinematic viscosity, and κ_\perp is the perpendicular thermal diffusivity. The instability occurs at value $R = R_c \sim 1708$, independent of the fluid under consideration [5]. Taking into account that the thickness of the LC channel d up to $\sim 5 \mu\text{m}$, in our case $R \ll R_c$, and the driving force is weak enough to set up convection via the Rayleigh-Benard mechanism. We assume that the heat current satisfies Fourier's law and consider a LC system composed of asymmetric polar molecules, such as *cyanobiphenyl*, which are confined in the microsized LC volume.

Recently, a new method to control LC flow dynamics using a bidirectionally aligned liquid crystal (BALC) film was proposed [6]. It was shown for the case of bistable twisted nematic devices, that dynamic flow is essential to the switching mechanism [7] and the orientational defects on the restricted surfaces play a crucial role in the formation of the vortical flows. Taking into account that the potential applications of these LC materials are included, for instance, in the novel optothermal tweezers, more research is needed.

In order to elucidate the role of both the orientational defect and the heat flux \mathbf{q}^b directed at an angle α across the lower bounding surface in the formation of the vortical flow in the LC volume, we have analyzed the response of the LC material confined in the microsized 2D volume on the effect of the laser beam focused on the bounding surface.

*Corresponding author: alexandre.zakharov@yahoo.ca;

www.ipme.ru

†pashamaslennikov@mail.ru

II. FORMULATION OF THE RELEVANT EQUATIONS FOR NEMATIC FLUIDS

We consider the 2D nematic fluid composed of polar molecules, such as cyanobiphenyls, at density ρ , and delimited by two horizontal and two lateral surfaces at mutual distances $2D$ and $2d$, respectively. The coordinate system defined by our task assumes that the director $\hat{\mathbf{n}} = (n_x, 0, n_z) = \sin\theta\hat{\mathbf{i}} + \cos\theta\hat{\mathbf{k}}$ is in the xz plane, where $\hat{\mathbf{i}}$ is the unit vector directed parallel to the horizontal restricted surfaces, which coincides with the planar director orientation on the upper boundary ($\hat{\mathbf{i}}\|\hat{\mathbf{n}}_{z=d}$), whereas the unit vector $\hat{\mathbf{k}}$ is directed parallel to the lateral restricted surfaces, which coincides with the planar director orientation on these surfaces ($\hat{\mathbf{k}}\|\hat{\mathbf{n}}_{x=\pm d}$). Here, $\theta \equiv \theta(x, z, t)$ denotes the polar angle, i.e., the angle between the direction of the director $\hat{\mathbf{n}}$ and the unit vector $\hat{\mathbf{k}}$, and $\hat{\mathbf{j}} = \hat{\mathbf{k}} \times \hat{\mathbf{i}}$.

The aim of our paper is to analyze the nature of thermally excited vortical flow $\mathbf{v} = u\hat{\mathbf{i}} + w\hat{\mathbf{k}}$ in a microsized nematic volume under the influence of a heat flux \mathbf{q}^b directed across the lower bounding surface at an angle α with respect to the unit vector $\hat{\mathbf{i}}$. Here, $u \equiv v_x(x, z, t)$ and $w \equiv v_z(x, z, t)$ are the components of the vector \mathbf{v} . Taking into account that the width of the LC channel $d \sim 1\text{--}5\ \mu\text{m}$, one can assume the mass density ρ to be constant across the channel, and thus deal with an incompressible fluid. The incompressibility condition $\nabla \cdot \mathbf{v} = 0$ gives

$$u_{,x} + w_{,z} = 0, \quad (1)$$

where $u_{,x} = \frac{\partial u}{\partial x}$.

The hydrodynamic equations describing the nature of thermally excited vortical flow in the microsized nematic volume, when there exists the heat flux \mathbf{q}^b across the lower boundary, can be derived from the torque balance equation $\mathbf{T}_{\text{el}} + \mathbf{T}_{\text{vis}} + \mathbf{T}_{\text{tm}} = \mathbf{0}$, which has the form [2–4]

$$\left[\frac{\delta \mathcal{W}_F}{\delta \hat{\mathbf{n}}} + \frac{\delta \mathcal{R}^{\text{vis}}}{\delta \hat{\mathbf{n}}_t} + \frac{\delta \mathcal{R}^{\text{tm}}}{\delta \hat{\mathbf{n}}_t} \right] \times \hat{\mathbf{n}} = 0, \quad (2)$$

whereas the linear momentum equation can be written as [2–4]

$$\rho \frac{d\mathbf{v}}{dt} = \nabla \cdot \boldsymbol{\sigma}, \quad (3)$$

where $\boldsymbol{\sigma} = \boldsymbol{\sigma}^{\text{el}} + \boldsymbol{\sigma}^{\text{vis}} + \boldsymbol{\sigma}^{\text{tm}} - P\boldsymbol{\mathcal{E}}$ is the full stress tensor (ST), and $\boldsymbol{\sigma}^{\text{el}} = -\frac{\partial \mathcal{W}_F}{\partial \nabla \hat{\mathbf{n}}} \cdot (\nabla \hat{\mathbf{n}})^T$, $\boldsymbol{\sigma}^{\text{vis}} = \frac{\delta \mathcal{R}^{\text{vis}}}{\delta \nabla \mathbf{v}}$, and $\boldsymbol{\sigma}^{\text{tm}} = \frac{\delta \mathcal{R}^{\text{tm}}}{\delta \nabla \mathbf{v}}$ are the ST components corresponding to the elastic, viscous, and thermomechanical forces, respectively (see the Appendix). Here, $\mathcal{R} = \mathcal{R}^{\text{vis}} + \mathcal{R}^{\text{tm}} + \mathcal{R}^{\text{th}}$ is the full Rayleigh dissipation function composed of the viscous, thermomechanical and thermal contributions (for details, see the Appendix), $\mathcal{W}_F = \frac{1}{2}[K_1(\nabla \cdot \hat{\mathbf{n}})^2 + K_3(\hat{\mathbf{n}} \times \nabla \times \hat{\mathbf{n}})^2]$ denotes the elastic energy density, K_1 and K_3 are splay and bend elastic coefficients, P is the hydrostatic pressure, and $\boldsymbol{\mathcal{E}}$ is the unit tensor. When a temperature gradient ∇T is set up across the LC channel, we expect the temperature field $T(x, z, t)$ satisfies the heat conduction equation [2–4]

$$\rho C_P \frac{dT}{dt} = \nabla \cdot \mathbf{q}, \quad (4)$$

where $\mathbf{q} = T \frac{\delta \mathcal{R}}{\delta \nabla T}$ is the heat flux in the LC channel, and C_P is the heat capacity of the LC system.

We will also examine the effect of the orientational defect (OD) on the formation of the vortical flow \mathbf{v} excited in the nematic volume under influence of the temperature gradient $\nabla T(x, z, t)$, which is initiated by the focused laser beam on the lower restricted surface. That defect is characterized by continuously changing the director's orientation along the length of the lower restricted surface, from the homeotropic to planar, and again to homeotropic orientation. So, our 2D aligned nematic state with the orientational defect contains a gradient of $\nabla\theta$ on the lower boundary, i.e.,

$$\theta_{-10 \leq x \leq -L, z=-1} = \theta_{L \leq x \leq 10, z=-1} = 0, \quad \theta_{-L < x < L, z=-1} = \mathcal{A}, \quad (5)$$

and the planar orientation on the upper and lateral surfaces, i.e.,

$$\theta_{x=\pm 10, -1 < z < 1} = 0, \quad \theta_{-10 \leq x \leq 10, z=1} = \frac{\pi}{2}, \quad (6)$$

where $\mathcal{A} = \tan^{-1}(\frac{L^2 - x^2}{4x^4})$, $L = \frac{l}{d}$, and $2l$ is the length of the orientational defect on the lower boundary with the director's orientation changing continuously from the homeotropic to planar, and again to homeotropic orientation, whereas on the rest length of that surface there is the homeotropic director's orientation ($\hat{\mathbf{k}}\|\hat{\mathbf{n}}_{z=-1}$). Notice that in our calculations the ratio D/d is equal to 10. Moreover, we will work with the dimensionless space variables $\bar{x} = x/d$ and $\bar{z} = z/d$, and in the following equations the overbars will be eliminated.

In order to elucidate the role of both the orientational defect and the heat flux \mathbf{q}^b directed at an angle α across the lower bounding surface in the formation of the vortical flow we consider the hydrodynamic regime with the heat flux $\mathbf{q}^b = q_z \hat{\mathbf{k}} = Q \sin \alpha \hat{\mathbf{k}}$, where α is the angle between vectors $\hat{\mathbf{n}}$ and $\hat{\mathbf{i}}$. In the dimensionless form it can be written as [3]

$$(\chi_{,z}(x, z, \tau))_{z=-1} = \left[\frac{q_z - (\lambda - 1)n_x n_z \chi_{,x}}{\lambda n_z^2 + n_x^2} \right]_{z=-1}, \quad (7)$$

whereas on the rest boundaries the temperature is kept constant

$$\chi_{-10 \leq x \leq 10, z=1} = \chi_{x \pm 10, -1 < z < 1} = \chi_c. \quad (8)$$

Here, $Q = Q(x, z = -1, \tau)$ is the injected energy across the lower boundary, $q_z = Q \sin \alpha$, $\lambda = \lambda_{\parallel}/\lambda_{\perp}$, λ_{\parallel} and λ_{\perp} are the heat conductivity coefficient parallel and perpendicular to the director $\hat{\mathbf{n}}$, $\chi_{,x} = \frac{\partial \chi}{\partial x}$, $\chi \equiv \chi(x, z, \tau) = T(x, z, \tau)/T_{\text{NI}}$ is the dimensionless temperature, T_{NI} is the nematic-isotropic transition temperature, and $\tau = \frac{t}{t_R}$ is the dimensionless characteristic time needs for reorientation of the director $\hat{\mathbf{n}}$, respectively.

The velocity $\mathbf{v} = u\hat{\mathbf{i}} + w\hat{\mathbf{k}}$ on these surfaces has to satisfy the no-slip boundary condition

$$u_{-10 \leq x \leq 10, z=-1} = u_{x=\pm 10, -1 < z < 1} = 0, \quad w_{-10 \leq x \leq 10, z=-1} = w_{x \pm 10, -1 < z < 1} = 0. \quad (9)$$

With the aim to analyze the nature of thermally excited vortical flow in the microsized nematic volume under the influence of the heat flux \mathbf{q}^b directed across the lower bounding surface at an angle α with respect to the unit vector $\hat{\mathbf{i}}$, we consider the

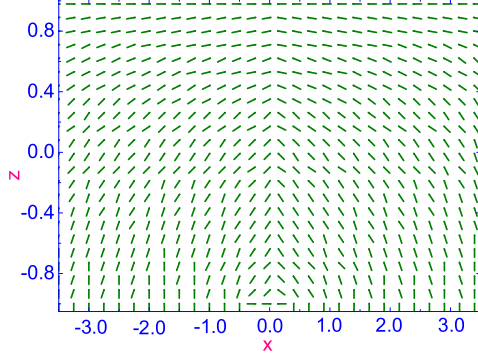


FIG. 1. The fragment of initial distribution of the director field $\hat{\mathbf{n}}_{\text{elast}}^{\text{eq}}(x, z)$ near the orientational defect located at $-L < x < L, z = -1$. Here, $L = \pm 0.5$.

dimensionless analog of balance equations. The dimensionless torque balance equation, corresponding to Eq. (2), has the form (for details, see the Appendix and Ref. [4])

$$\begin{aligned} n_z n_{x,\tau} - n_x n_{z,\tau} &= \delta_1 [n_z \mathcal{M}_{0,x} - n_x \mathcal{M}_{0,z} + K_{31} (n_z f_{,z} + n_x f_{,x})] \\ &\quad - \frac{1}{2} \psi_{,xx} [1 + \gamma_{21} (n_x^2 - n_z^2)] - \frac{1}{2} \psi_{,zz} [1 - \gamma_{21} (n_x^2 - n_z^2)] \\ &\quad \times 2\gamma_{21} \psi_{,xz} n_x n_z + \psi_{,z} \mathcal{N}_x + \mathcal{N}_z \psi_{,x} + \delta_2 (\chi_{,x} \mathcal{L}_{,x} + \chi_{,z} \mathcal{L}_{,z}), \end{aligned} \quad (10)$$

The dimensionless linear balance momentum equation, corresponding to Eq. (3), takes the form

$$\begin{aligned} \delta_3 \psi_{,xz\tau} &= a_1 \psi_{,zzzz} + a_2 \psi_{,xzzz} + a_3 \psi_{,xxzz} + a_4 \psi_{,xxxx} \\ &\quad + a_5 \psi_{,xxxx} + a_6 \psi_{,zzz} + a_7 \psi_{,xzz} + a_8 \psi_{,xvz} \\ &\quad + a_9 \psi_{,xxx} + a_{10} \psi_{,zz} + a_{11} \psi_{,xz} + a_{12} \psi_{,xx} + \mathcal{F}, \end{aligned} \quad (11)$$

where a_i ($i = 1, \dots, 12$) and \mathcal{F} are functions that have been defined in the Appendix of Ref. [4]. The dimensionless entropy balance equation, corresponding to Eq. (4), can be

written as

$$\begin{aligned} \chi_{,\tau} &= [\chi_{,x} (\lambda n_x^2 + n_z^2) + (\lambda - 1) n_x n_z \chi_{,z}]_{,x} \\ &\quad + [\chi_{,z} (\lambda n_z^2 + n_x^2) + (\lambda - 1) n_x n_z \chi_{,x}]_{,z} \\ &\quad + \delta_4 \chi \left(\nabla \cdot \frac{\partial \mathcal{R}^{\text{tm}}}{\partial \nabla \chi} \right) - \psi_{,z} \chi_{,x} + \psi_{,x} \chi_{,z}, \end{aligned} \quad (12)$$

where $\tau = \frac{t}{t_T}$ is the dimensionless time, $t_T = \frac{\rho C_p d^2}{\lambda_{\perp}}$, $\bar{\psi} = \frac{t_T}{d^2} \psi$ is the scaled analog of the stream function ψ for the velocity field $\mathbf{v} = u\hat{\mathbf{i}} + w\hat{\mathbf{k}} = -\nabla \times \hat{\mathbf{j}}\psi$ (see Ref. [4]), $f = n_{x,z} - n_{z,x}$, $n_{z,\tau} = \frac{\partial n_z}{\partial \tau}$, $\mathcal{M}_0 = \nabla \cdot \hat{\mathbf{n}}$, $\mathcal{N}_z = n_z n_{x,z} - n_x n_{z,z}$, $\mathcal{L}_x = n_x n_{z,x} - \frac{3}{2} n_z n_{x,x} + \frac{1}{2} n_x n_{x,z}$, $\mathcal{L}_z = -n_z n_{x,z} + \frac{3}{2} n_x n_{z,z} - \frac{1}{2} n_z n_{z,x}$. Notice that the overbars in the stream function ψ have been (and will be) eliminated in the last as well as in the following equations. The dimensionless thermomechanical contribution to the total Rayleigh dissipation function \mathcal{R}^{tm} can be written as (for the details, see the Appendix and Refs. [3,4]) $\mathcal{R}^{\text{tm}} = \chi_{,x} (-\frac{1}{2} n_z \mathcal{M}_0 - n_z M_{xx} + n_x^2 (n_x M_{zz} - M_{xx} n_z + 2n_x M_{xz})) + \chi_{,z} (\frac{1}{2} n_x \mathcal{M}_0 + n_x M_{zz} + n_z^2 (n_x M_{zz} - M_{xx} n_x - 2n_z M_{xz}))$. Here, M_{ij} ($i, j = x, z$) are components of the tensor $\mathbf{M} = \frac{1}{2} [\nabla \hat{\mathbf{n}} + (\nabla \hat{\mathbf{n}})^T]$. The function $\mathcal{F} = (\sigma_{xx}^{\text{el}} + \sigma_{xx}^{\text{tm}} - \sigma_{zz}^{\text{el}} - \sigma_{zz}^{\text{tm}})_{,xz} + (\sigma_{xz}^{\text{el}} + \sigma_{zx}^{\text{tm}})_{,zz} - (\sigma_{xz}^{\text{el}} + \sigma_{xz}^{\text{tm}})_{,xx}$, the coefficients a_i ($i = 1, \dots, 12$), the functions $\sigma_{ij}^{\text{tm}}(i, j = x, z)$ and $\sigma_{ij}^{\text{el}}(i, j = x, z)$ are given in the Appendix of Ref. [4]. The set of parameters of the LC system are $K_{31} = \frac{K_3}{K_1}$, $\gamma_{21} = \frac{\gamma_2}{\gamma_1}$, $\delta_1 = \frac{t_T K_1}{\gamma_1 d^2}$, $\delta_2 = \frac{\rho C_p T_{NI} \xi}{\lambda_{\perp} \gamma_1}$, $\delta_3 = \frac{\rho d^2}{\gamma_1 t_T}$, and $\delta_4 = \frac{\xi}{\lambda_{\perp} t_T}$. Here, $\xi = 10^{-12} [J/mK]$ is the thermomechanical constant [2,4,8].

Now, the reorientation of the director in the LC volume confined between two horizontal and two vertical solid surfaces, when the relaxation regime is governed by the viscous, elastic, and thermomechanical forces, and with accounting for the flow, can be obtained by solving the system of the nonlinear partial differential equations (10), (11), and (12) with the appropriate dimensionless boundary conditions for the polar angle θ -Eqs. (5)–(6)], or for the director field $\hat{\mathbf{n}}$, stream function ψ and temperature χ , and initial conditions. The boundary conditions at the solid surfaces can be written

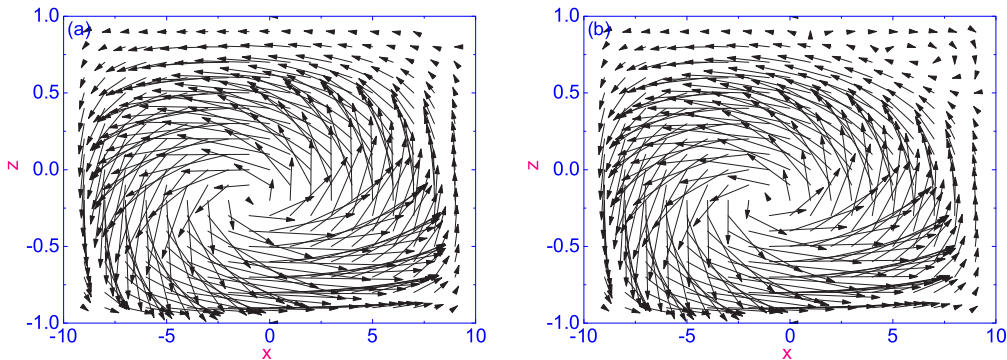
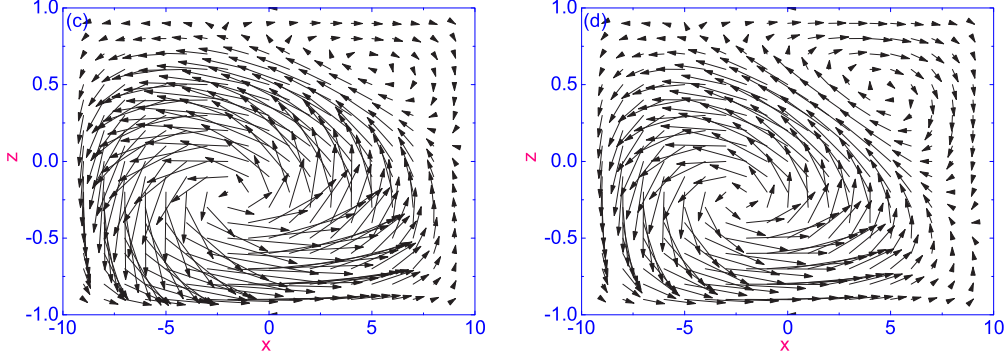


FIG. 2. Distribution of the velocity field $\mathbf{v} = u\hat{\mathbf{i}} + w\hat{\mathbf{k}}$ in the microscopic nematic volume with the orientational defect located at $-L \leq x \leq L, z = -1$, when the heat flux \mathbf{q}^b is directed at two values of the angle α : (a) 20° and (b) 40° , respectively. The heating occurs during time $\tau_{\text{in}} = 1.6 \times 10^{-4}$ (~ 0.29 ms), whereas the value of the dimensionless heat flux coefficient \mathcal{Q}_0 is equal to 0.05. Here, 1 mm of the arrow length is equal to $1.8 \mu\text{m/s}$.

FIG. 3. Same as in Fig. 2, but the values of the angle α are (c) 60° and (d) 80° , respectively.

as

$$\begin{aligned}
 (n_x)_{x=\pm 10, -1 \leq z \leq 1} &= 0, & (n_x)_{-10 < x < 10, z=1} &= 1, \\
 (n_x)_{-10 < x < -L, z=-1} &= (n_x)_{L < x < 10, z=-1} = 0, & (n_x)_{-L < x < L, z=-1} &= \sin \mathcal{A}, \\
 \chi_{x=\pm 10, -1 \leq z \leq 1} &= 0.97, & \chi_{-10 < x < 10, z=1} &= 0.97, \\
 (\chi_{,z}(x, z, \tau))_{z=-1} &= \left[\frac{q_z - (\lambda - 1)n_x n_z \chi_{,x}}{\lambda n_z^2 + n_x^2} \right]_{z=-1}, \\
 (\psi_{,x})_{x=\pm 10, -1 \leq z \leq 1} &= (\psi_{,z})_{x=\pm 10, -1 \leq z \leq 1} = 0, \\
 (\psi_{,x})_{-10 \leq x \leq 10, z=-1} &= (\psi_{,z})_{-10 \leq x \leq 10, z=-1} = 0, \quad (13)
 \end{aligned}$$

whereas the initial condition takes the form

$$\hat{\mathbf{n}}(x, z, \tau = 0) = \hat{\mathbf{n}}_{\text{elast}}^{\text{eq}}(x, z). \quad (14)$$

Recently, laser-induced heating was used to inject energy \mathcal{Q} across the bounding surface at the microscopic scale [3,4]. In our case the LC sample will be heated by a laser beam, focused, for instance, on the lower boundary ($z = -1, x = x_0$), and the dimensionless injected energy \mathcal{Q} can be written as

$$\mathcal{Q} = \mathcal{Q}_0 \exp\left(-2 \frac{(x - x_0)^2 + (z - z_0)^2}{\Delta^2}\right) \mathcal{H}[\tau_{\text{in}} - \tau], \quad (15)$$

where $\Delta = \frac{\omega_0}{d} = 2L$ is the dimensionless Gaussian spot size, $\mathcal{H}[\tau_{\text{in}} - \tau]$ is the Heaviside step function, τ_{in} is the duration of the energy injection into the nematic volume, and x_0 and z_0 are the dimensionless positions of the laser focus, and $\mathcal{Q}_0 = \frac{2}{\pi \Delta} \frac{d^2 P}{\lambda_1 T_{Nl}}$ is the dimensionless heat flux coefficient. Here, P is the laser power and ω is the Gaussian spot size, respectively.

For the case of 4-cyano-4'-pentylbiphenyl (5CB), at temperatures corresponding to nematic phase, the set of parameters, involved in Eqs. (10)–(12), are $\delta_1 \sim 10^{-3}$, $\delta_2 \sim 0.3$, $\delta_3 \sim 10^{-6}$, and $\delta_4 \sim 10^{-4}$.

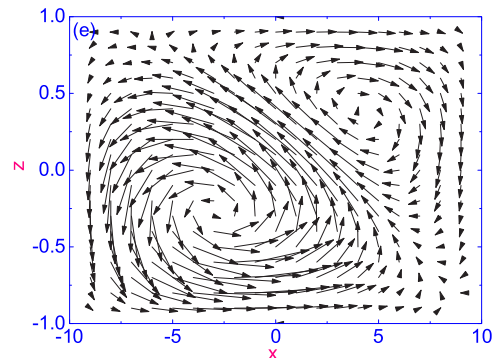
Using the fact that $\delta_3 \ll 1$, the Navier-Stokes [Eq. (11)] equation can be considerably simplified. Thus, the whole left-hand side of Eq. (11) can be neglected and that equation take the form

$$\begin{aligned}
 a_1 \psi_{,zzzz} + a_2 \psi_{,xzzz} + a_3 \psi_{,xxzz} + a_4 \psi_{,xxxz} + a_5 \psi_{,xxxx} \\
 + a_6 \psi_{,zzz} + a_7 \psi_{,xzz} + a_8 \psi_{,xxz} + a_9 \psi_{,xxx} + a_{10} \psi_{,zz} \\
 + a_{11} \psi_{,xz} + a_{12} \psi_{,xx} + \mathcal{F} = 0, \quad (16)
 \end{aligned}$$

where a_i ($i = 1, \dots, 12$) and \mathcal{F} are the functions defined in Refs. [3,4].

III. CALCULATIONAL PROCEDURE AND RESULTS

Now, the nematic phase confined in the microsized volume is heated by the laser beam focused on the lower bounding surface at the angle α with respect to the unit vector $\hat{\mathbf{i}}$. We will also examine the effect of coupling between the gradient of the director field $\nabla \hat{\mathbf{n}}$ and $\nabla \chi$ on the formation of the vortical flow inside the nematic volume. Note that the magnitude \mathcal{Q}_0 and duration τ_{in} of the heat injected across the lower boundary are restricted only by the nematic phase stability condition. On the other hand, when the director $\hat{\mathbf{n}}$ is strongly homogeneously anchored to the upper and two lateral surfaces, and with the orientational defect on the lower boundary, the director field $\hat{\mathbf{n}}(x, z, \tau)$ has to satisfy the boundary conditions Eq. (13) and its initial orientation is chosen equal to $\hat{\mathbf{n}}(x, z, \tau = 0) = \hat{\mathbf{n}}_{\text{elast}}^{\text{eq}}(x, z)$. Here, $\hat{\mathbf{n}}_{\text{elast}}^{\text{eq}}(x, z)$ is the equilibrium distribution of the director field over the nematic volume obtained from Eq. (10) with $\psi_{,x} = \psi_{,z} = \chi_{,x} = \chi_{,z} = 0$, and with the boundary conditions in the form of Eq. (13), whereas the initial condition is chosen in the form $\theta_{\text{elast}}(x, z, \tau = 0) = 0$, at $x = \pm 10$, and $-1 \leq z \leq 1$; $\frac{\pi}{4}(z+1)$, at $-10 < x < -L$, and $L < x < 10$; $\frac{\pi}{2}$, at $-L \leq x \leq L$, and $z = -1$, respectively. Notice that the initial distribution of the director field $\hat{\mathbf{n}}_{\text{elast}}^{\text{eq}}(x, z)$ over the microsized volume has been obtained from Eq. (10) by means of relaxation method [9]. In the calculations, the relaxation criterion $\epsilon = |(\theta_{(m+1)}(x, z, \tau) -$

FIG. 4. Same as in Fig. 2, but the value of the angle α is equal to 90° .

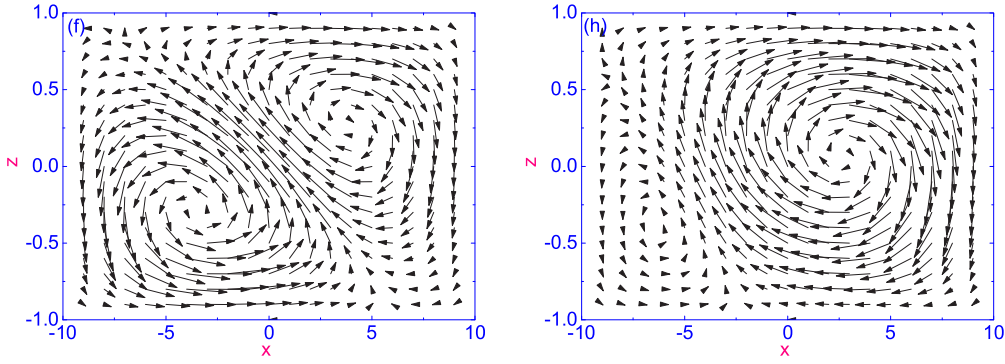


FIG. 5. Same as in Fig. 2, but the values of the angle α are (f) 100° and (h) 120° , respectively.

$\theta_{(m)}(x, z, \tau)/\theta_{(m)}(x, z, \tau)$ was chosen to be equal to 10^{-4} , and the numerical procedure was then carried out until a prescribed accuracy was achieved. Here, m is the iteration number.

Figure 1 shows a fragment of the initial distribution of the director field $\hat{\mathbf{n}}_{\text{elast}}^{\text{eq}}(x, z)$ near the orientational defect located at $-L < x < L, z = -1$. Here, $L = \pm 0.5$ are the right and left ends of the orientational defect on the lower boundary. According to our calculations the highest value of $|\nabla \hat{\mathbf{n}}(x, z)|$ is reached in the vicinity of the orientational defect and its effect extends up to $3/4$ of the thickness of the nematic volume.

In turn, the initial distribution of the temperature field $\chi(x, z, \Delta\tau)$, corresponding to the first time step $\Delta\tau$, has been obtained from Eq. (12), by means of the relaxation method with $\psi_{,x} = \psi_{,z} = 0$ and with the boundary and initial conditions in the form of Eqs. (13)–(14). Having obtained both the initial distributions of the director and the temperature fields, as well as the function \mathcal{F} , which is involved in Eq. (16), one can calculate the initial distribution of the stream function $\psi(x, z, \Delta\tau)$, corresponding to the first time step $\Delta\tau$. The next time step $\Delta\tau$ for the velocity and temperature fields, as well as for the director's distribution across the nematic volume is initiated by the sweep method [10].

The stability of the numerical procedure for Eqs. (10), (12), and (16) was defined by the conditions [9]:

$$\frac{\Delta\tau}{\delta_3} \left(\frac{1}{(\Delta x)^2} + \frac{1}{(\Delta z)^2} \right) \leq \frac{1}{2}, \quad \frac{3a_5}{(\Delta x)^4} - \frac{2a_1}{(\Delta z)^4} > 0,$$

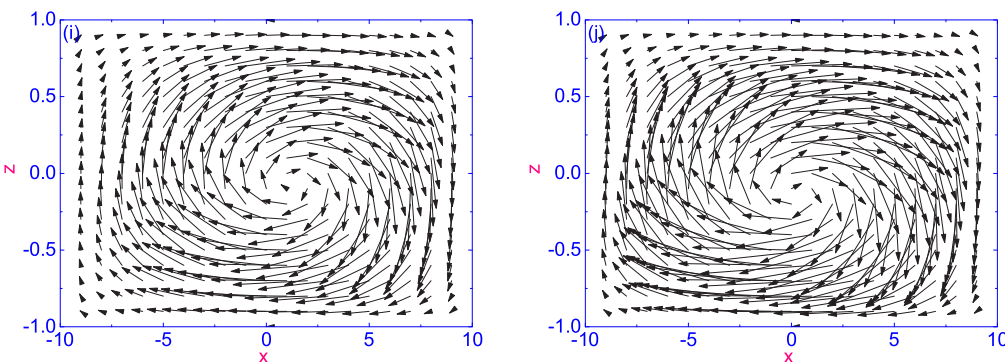


FIG. 6. Same as in Fig. 2, but the values of the angle α are (i) 140° and (j) 160° , respectively.

where Δx and Δz are the space steps in the x and z directions, and a_1 and a_5 are the coefficients defined in Eq. (16). Now we can calculate the evolution of both the velocity $\mathbf{v} = u\hat{\mathbf{i}} + w\hat{\mathbf{k}}$ and the temperature $\chi(x, z, \tau = \tau_{\text{in}})$ fields over the nematic volume with the orientational defect as the function of the angle α . Distribution of the velocity field \mathbf{v} in the microscopic nematic volume with the orientational defect located at $-L \leq x \leq L, z = -1$, when the laser beam is directed at the values of the angle α equal to 20° and 40° [Figs. 2(a) and 2(b)], 60° and [Figs. 3(c) and 3(d)], 90° [Fig. 4(e)], 100° and 120° [Figs. 5(f) and 5(h)], 140° and 160° [Figs. 6(i) and 6(j)] are shown in Figs. 2, 3, 4, 5, and 6, respectively. The heating occurs during time $\tau_{\text{in}} = 1.6 \times 10^{-4}$ (~ 0.29 ms), whereas the value of dimensionless heat flux coefficient \mathcal{Q}_0 is equal to 0.05. The distribution of the velocity field \mathbf{v} in the microscopic nematic volume with the orientational defect located at $-L \leq x \leq L, z = -1$, when the heat flux \mathbf{q}^b is directed at two values of the angle $\alpha = 20^\circ$ and 40° , with respect to the lower bounding surface is characterized by maintaining vortices as shown in Figs. 2(a) and 2(b), respectively. Here, 1 mm of the arrow length is equal to $1.8 \mu\text{m/s}$. The direction and magnitude of the hydrodynamic flow $\mathbf{v}(x, z, \tau)$ is influenced by both the direction of the heat flux \mathbf{q}^b across the lower bounding surface and the character of the orientational defect. According to our calculations of the director field $\hat{\mathbf{n}}(x, z, \tau)$ across the nematic volume, the highest value of $|\nabla \hat{\mathbf{n}}(x, z)|$ is reached in the vicinity of the orientational defect, and, as a result, the biggest thermally excited velocities occur in the vicinity of the lower hotter surface. In that case, the self-sustaining vortical flow is excited in the negative sense

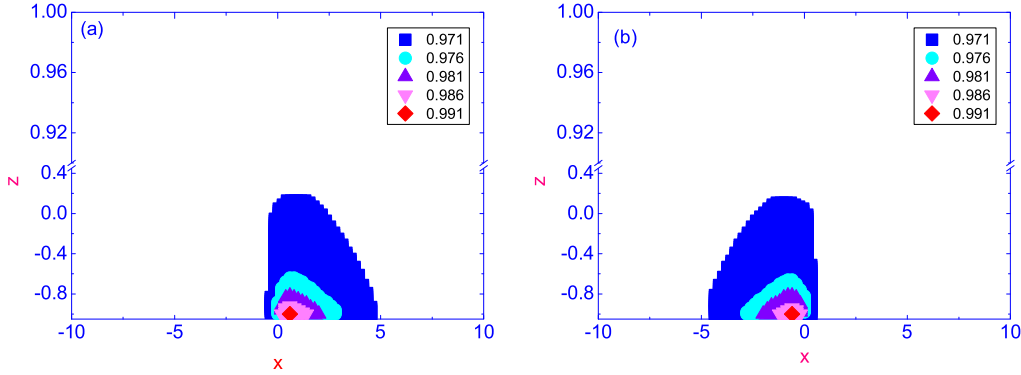


FIG. 7. Plot of the temperature field distribution $\chi(x, z, \tau = \tau_{\text{in}})$ over the nematic volume near the orientational defect located at $-L \leq x \leq L, z = -1$, when the heat flux \mathbf{q}^b is directed at two values of the angle α : (a) 20° and (b) 160° , respectively. The heating occurs during time $\tau_{\text{in}} = 1.6 \times 10^{-4}$ (~ 0.29 ms), whereas the value of the dimensionless heat flux coefficient Q_0 is equal to 0.05.

(counterclockwise) around its center, as the value of the angle α reaches 60° . Further increase in the angle value of more than 60 degrees leads to the formation of two vortices, one, larger, in the left-hand side of the nematic volume, and another, smaller, in the right-hand side of the LC phase, as shown in Figs. 3(c) and 3(d), 4(e), and 5(f) and 5(h), respectively. With increasing the value of the angle α , the larger vortex begins to decrease in size, while the smaller vortex begins to increase. The size of the smaller vortex reaches its maximum size at the angle $\alpha = 120^\circ$ [see Fig. 5(h)]. Notice that the bigger self-sustaining vortical flow in the left-hand side of the LC volume is thermally excited in the negative sense (counterclockwise), whereas the smaller vortical flow in the right-hand side of the LC volume is excited in the positive sense (clockwise) around their centers. With increasing the value of the angle α more than 120 degrees, the larger vortex disappears and we have only one the self-sustaining vortical flow in the positive sense (clockwise) around its center [see Figs. 6(i) and 6(j)].

So, based on our calculations, one can conclude that the direction of the heat flux across the hotter bounding surface with the orientational defect plays a crucial role in maintaining the thermally excited vortical flow in the 2D LC cell.

The distribution of the temperature field $\chi(x, z, \tau = \tau_{\text{in}})$ over the nematic volume near the orientational defect located at $-L \leq x \leq L, z = -1$, when the heat flux \mathbf{q}^b is directed at two values of the angle α : 20° [Fig. 7(a)] and 160° [Fig. 7(b)], after time term $\tau_{\text{in}} = 1.6 \times 10^{-4}$ (~ 0.29 ms), is shown in Fig. 7. The value of the dimensionless heat flux coefficient Q_0 is equal to 0.05 ($\sim 4.2 \times 10^{-4}$ mW/ μm^2). In general, under the above conditions, the picture of warming is such that only a small part of the nematic phase is involved in the heating process, while a large part of the volume of the fluid were not heated. It should be noted that in both cases the area of the greatest heating was shifted in the direction in which the heat flux was directed due to laser radiation.

IV. CONCLUSION

We have investigated the reorientational dynamics in the case of a hybrid-oriented two-dimensional (2D) liquid crystal (LC) cell, under the influence of a temperature gradient ∇T , caused by a heat flux \mathbf{q} directed at an angle α across the lower bounding surface with the orientational defect. Our

calculations, based on the appropriate nonlinear extension of the Ericksen-Leslie theory, accounting for the entropy balance equation, show that due to interaction between ∇T and the gradient of the director field $\nabla \hat{\mathbf{n}}$ in the LC sample with the orientational defect on the lower hotter boundary is excited in the vortical flow. The direction and magnitude of the hydrodynamic flow has influenced both the direction of the heat flux \mathbf{q}^b across the lower bounding surface and the character of the orientational defect. Our calculations show that the biggest thermally excited velocity occurs in the vicinity of the orientational defect. The analysis showed that at the same power of the laser radiation, with a change in the value of the angle α , the picture of the vortex flow in the LC cell changes. When the heat flux \mathbf{q}^b is directed at the angle α less than 40 degrees, the LC volume is excited on the self-sustaining vortical flow in the negative sense (counterclockwise) around its center. Further increase in the angle value of more than 60 degrees leads to the formation of two vortices, one larger, in the left-hand side of the LC volume, another smaller, in the right-hand side of the LC volume, respectively. With increasing the value of the angle α up to right angle and more, the larger vortex begins to decrease in size, while the smaller vortex reaches its maximum size at the angle 120 degrees. An increase in the angle value of more than 120 degrees leads to the formation of one of the self-sustaining vortical flows in the positive sense (clockwise) around its center.

Recently, the vortical flow formation in homeotropically oriented LC film doped by chiral molecules has been observed [11]. It has been shown, by means of circular polarization techniques, that in the LC film, due to the pumping of energy by laser irradiation, the vortical flow is excited similar to what is shown in Figs. 2–6. The experimentally observed formation of the vortical flow in the LC film has been ascribed to thermocapillary convection in the LC sample. In turn, in our case, the vortical flow is excited due to coupling between director and temperature gradients, initiated by the laser beam irradiation.

So, based on our calculations, one can conclude that the direction of the heat flux across the bounding surface with the orientational defect plays a crucial role in maintaining the thermally excited vortical flow in the 2D LC cell, and is expected to be applied for novel opto-thermal tweezers.

ACKNOWLEDGMENTS

We acknowledge financial support of the Russian Funds for Fundamental Research (Grant No. 16-02-00041-a) and of the Ministry of Education and Science of the Russian Federation (Grants No. 3.11888.2018/11.12 and 3.9585.2017/8.9).

APPENDIX: TORQUES, STRESS TENSOR COMPONENTS AND ENTROPY BALANCE EQUATION

The hydrodynamic equations describing the reorientation of the LC phase in 2D case, when the system is subjected to a temperature gradient ∇T , due to the heat flux \mathbf{q}^b across the lower restricted surface, can be derived from the torque balance equation [2–4]

$$\mathbf{T}_{\text{el}} + \mathbf{T}_{\text{vis}} + \mathbf{T}_{\text{tm}} = \mathbf{0},$$

where $\mathbf{T}_{\text{el}} = \frac{\delta \mathcal{W}_{\text{el}}}{\delta \hat{\mathbf{n}}} \times \hat{\mathbf{n}}$ is the elastic, $\mathbf{T}_{\text{vis}} = \frac{\delta \mathcal{R}^{\text{vis}}}{\delta \hat{\mathbf{n}}} \times \hat{\mathbf{n}}$ is the viscous, and $\mathbf{T}_{\text{tm}} = \frac{\delta \mathcal{R}^{\text{tm}}}{\delta \hat{\mathbf{n}}} \times \hat{\mathbf{n}}$ is the thermomechanical torques, respectively. The linear momentum equation for the velocity field \mathbf{v} can be written as [2–4]

$$\rho \frac{d\mathbf{v}}{dt} = \nabla \cdot \boldsymbol{\sigma},$$

where $\frac{d\mathbf{v}}{dt} = \frac{\partial \mathbf{v}}{\partial t} + u\mathbf{v}_{,x} + w\mathbf{v}_{,z}$, $\boldsymbol{\sigma} = \boldsymbol{\sigma}^{\text{el}} + \boldsymbol{\sigma}^{\text{vis}} + \boldsymbol{\sigma}^{\text{tm}} - \mathcal{P}\mathcal{E}$ is the full stress tensor (ST), and $\boldsymbol{\sigma}^{\text{el}} = -\frac{\partial \mathcal{W}_{\text{el}}}{\partial \nabla \hat{\mathbf{n}}} \cdot (\nabla \hat{\mathbf{n}})^{\text{T}}$, $\boldsymbol{\sigma}^{\text{vis}} = \frac{\delta \mathcal{R}^{\text{vis}}}{\delta \nabla \hat{\mathbf{n}}}$, and $\boldsymbol{\sigma}^{\text{tm}} = \frac{\delta \mathcal{R}^{\text{tm}}}{\delta \nabla \hat{\mathbf{n}}}$ are the ST components corresponding to the elastic, viscous, and thermomechanical forces, respectively. Here, $\mathcal{R} = \mathcal{R}^{\text{vis}} + \mathcal{R}^{\text{tm}} + \mathcal{R}^{\text{th}}$ is the full Rayleigh dissipation function, $\mathcal{W}_{\text{el}} = \frac{1}{2}[K_1(\nabla \cdot \hat{\mathbf{n}})^2 + K_3(\hat{\mathbf{n}} \times \nabla \times \hat{\mathbf{n}})^2]$ denotes the elastic energy density, K_1 and K_3 are splay and bend elastic coefficients, \mathcal{P} is the hydrostatic pressure in the HALC system, and \mathcal{E} is the unit tensor. When the temperature gradient ∇T is set up, for instance, due to the heat flux \mathcal{O} across the lower restricted surface, we expect that the temperature field $T(x, z, t)$ satisfies the heat conduction equation [4]

$$\rho C_P \frac{dT}{dt} = -\nabla \cdot \mathbf{q},$$

where $\mathbf{q} = -T \frac{\delta \mathcal{R}}{\delta \nabla T}$ denotes the heat flux in the LC system and C_P is the heat capacity of the LC system.

The torque balance equation can be derived from the dimension balance of elastic $\mathbf{T}_{\text{el}} = \frac{\delta \mathcal{W}_{\text{el}}}{\delta \hat{\mathbf{n}}} \times \hat{\mathbf{n}}$, viscous $\mathbf{T}_{\text{vis}} = \frac{\delta \mathcal{R}^{\text{vis}}}{\delta \hat{\mathbf{n}}} \times \hat{\mathbf{n}}$, and thermomechanical $\mathbf{T}_{\text{tm}} = \frac{\delta \mathcal{R}^{\text{tm}}}{\delta \hat{\mathbf{n}}} \times \hat{\mathbf{n}}$ torques, where $\mathcal{W}_{\text{el}} = \frac{1}{2}[K_1(\nabla \cdot \hat{\mathbf{n}})^2 + K_3(\hat{\mathbf{n}} \times \nabla \times \hat{\mathbf{n}})^2]$ is the elastic energy, and K_1 and K_3 are the splay and bend elastic coefficients, $\hat{\mathbf{n}}_t \equiv \frac{d\hat{\mathbf{n}}}{dt}$ is the material derivative of $\hat{\mathbf{n}} = n_x \hat{\mathbf{i}} +$

$n_z \hat{\mathbf{k}}$, whereas $\mathcal{R}^{\text{vis}} = \alpha_1(\hat{\mathbf{n}} \cdot \mathbf{D}_s \cdot \hat{\mathbf{n}})^2 + \gamma_1(\hat{\mathbf{n}}_t - \mathbf{D}_a \cdot \hat{\mathbf{n}})^2 + 2\gamma_2(\hat{\mathbf{n}}_t - \mathbf{D}_a \cdot \hat{\mathbf{n}}) \cdot (\mathbf{D}_s \cdot \hat{\mathbf{n}} - (\hat{\mathbf{n}} \cdot \mathbf{D}_s \cdot \hat{\mathbf{n}})\hat{\mathbf{n}}) + \alpha_4 \mathbf{D}_s : \mathbf{D}_s + (\alpha_5 + \alpha_6)(\hat{\mathbf{n}} \cdot \mathbf{D}_s \cdot \mathbf{D}_s \cdot \hat{\mathbf{n}})$ is the viscous contribution to the total Rayleigh dissipation function $\mathcal{R} = \mathcal{R}^{\text{vis}} + \mathcal{R}^{\text{tm}} + \mathcal{R}^{\text{th}}$. Here, $\frac{1}{\xi} \mathcal{R}^{\text{tm}} = (\hat{\mathbf{n}} \cdot \nabla T) \mathbf{D}_s : \mathbf{M} + \nabla T \cdot \mathbf{D}_s \cdot \mathbf{M} \cdot \hat{\mathbf{n}} + (\hat{\mathbf{n}} \cdot \nabla T)(\hat{\mathbf{n}}_t - \mathbf{D}_a \cdot \hat{\mathbf{n}} - 3\mathbf{D}_s \cdot \hat{\mathbf{n}} + 3(\hat{\mathbf{n}} \cdot \mathbf{D}_s \cdot \hat{\mathbf{n}})\hat{\mathbf{n}}) \cdot \mathbf{M} \cdot \hat{\mathbf{n}} + \hat{\mathbf{n}}(\nabla \mathbf{v})^{\text{T}} \cdot \mathbf{M} \cdot \nabla T + \frac{1}{2}(\hat{\mathbf{n}} \cdot \mathbf{D}_s \cdot \hat{\mathbf{n}}) \nabla T \cdot \mathbf{M} \cdot \hat{\mathbf{n}} + \hat{\mathbf{n}}_t \cdot \mathbf{M} \cdot \nabla T + \frac{1}{2} \mathcal{M}_0 \nabla T \cdot \nabla \mathbf{v} \cdot \hat{\mathbf{n}} + (\hat{\mathbf{n}} \cdot \nabla T) \mathcal{M}_0 (\hat{\mathbf{n}} \cdot \mathbf{D}_s \cdot \hat{\mathbf{n}}) + \frac{1}{2} \mathcal{M}_0 \hat{\mathbf{n}}_t \cdot \nabla T$ and $\mathcal{R}^{\text{th}} = \frac{1}{T}(\lambda_{\parallel}(\hat{\mathbf{n}} \cdot \nabla T))^2 + \lambda_{\perp}(\nabla T - \hat{\mathbf{n}}(\hat{\mathbf{n}} \cdot \nabla T))^2$ are the thermomechanical and thermal contributions to \mathcal{R} , respectively. Here, α_1 – α_6 are the Leslie viscosity coefficients, $\gamma_1(T)$ and $\gamma_2(T)$ are the rotational viscosity coefficients (RVCs), ξ is the thermomechanical constant, and λ_{\parallel} , λ_{\perp} are the heat conductivity coefficients parallel and perpendicular to the director $\hat{\mathbf{n}}$, respectively. Here, $\mathbf{D}_s = \frac{1}{2}[\nabla \mathbf{v} + (\nabla \mathbf{v})^{\text{T}}]$ and $\mathbf{D}_a = \frac{1}{2}[\nabla \mathbf{v} - (\nabla \mathbf{v})^{\text{T}}]$ are the symmetric and asymmetric contributions to the rate of strain tensor, $\mathbf{M} = \frac{1}{2}[\nabla \hat{\mathbf{n}} + (\nabla \hat{\mathbf{n}})^{\text{T}}]$, and $\mathcal{M}_0 = \nabla \cdot \hat{\mathbf{n}}$ is the scalar invariant of the tensor \mathbf{M} . We use here the invariant, multiple dot convention: $\mathbf{a}\mathbf{b} = a_i b_j$, $\mathbf{a} \cdot \mathbf{b} = a_i b_i$, $\mathbf{A} \cdot \mathbf{B} = A_{ik} B_{kj}$, and $\mathbf{A} : \mathbf{B} = A_{ik} B_{ki}$, where repeated Cartesian indices are summed. Straightforward calculations for the geometry $\hat{\mathbf{n}} = (n_x, 0, n_z)$ give the dimensionless expressions for the elastic \mathbf{T}_{el} , viscous \mathbf{T}_{vis} and thermomechanical \mathbf{T}_{tm} contributions to the torque balance equation, as well as to the ST $\boldsymbol{\sigma}$ components and the entropy balance equation.

The dimensionless analog of the elastic, viscous, and thermomechanical contributions to the torque balance equation, as well as of the stress tensor components are given in Ref. [4], whereas the dimensionless analog of the heat flux $\mathbf{q} = -T \frac{\delta \mathcal{R}}{\delta \nabla T}$ is given by

$$-q_x = \chi_{,x}(\lambda n_x^2 + n_z^2) + (\lambda - 1)n_x n_z \chi_{,z} + \delta_4 \nabla_x \left(\chi \frac{\partial \mathcal{R}^{\text{tm}}}{\partial \nabla \chi} \right),$$

$$-q_z = \chi_{,z}(\lambda n_z^2 + n_x^2) + (\lambda - 1)n_x n_z \chi_{,x} + \delta_4 \nabla_z \left(\chi \frac{\partial \mathcal{R}^{\text{tm}}}{\partial \nabla \chi} \right).$$

Finally, the dimensionless entropy balance equation takes the form

$$\begin{aligned} \chi_{,\tau} &= [\chi_{,x}(\lambda n_x^2 + n_z^2) + (\lambda - 1)n_x n_z \chi_{,z}]_{,x} \\ &+ [\chi_{,z}(\lambda n_z^2 + n_x^2) + (\lambda - 1)n_x n_z \chi_{,x}]_{,z} \\ &+ \delta_4 \chi \left(\nabla \cdot \frac{\partial \mathcal{R}^{\text{tm}}}{\partial \nabla \chi} \right) - \psi_{,z} \chi_{,x} + \psi_{,x} \chi_{,z}, \end{aligned}$$

where ψ is the scaled analog of the current function for the velocity field $\mathbf{v} = u\hat{\mathbf{i}} + w\hat{\mathbf{k}} = -\nabla \times \hat{\mathbf{j}}\psi$.

[1] A. D. Rey, *Soft Matter* **6**, 3402 (2010).

[2] A. V. Zakharov and A. A. Vakulenko, *J. Chem. Phys.* **127**, 084907 (2007).

[3] A. V. Zakharov and A. A. Vakulenko, *Phys. Rev. E* **80**, 031711 (2009).

[4] A. V. Zakharov and P. V. Maslennikov, *Phys. Rev. E* **96**, 052705 (2017).

[5] C. Cross and P. C. Hohenberg, *Rev. Mod. Phys.* **65**, 851 (1993).

[6] Y. W. Li, C. Y. Lee, and H. S. Kwok, *Appl. Phys. Lett.* **94**, 061111 (2009).

- [7] A. V. Zakharov and A. A. Vakulenko, *Phys. Fluids* **24**, 073102 (2012).
- [8] R. S. Akopyan and B. Y. Zeldovich, *Sov. Phys. JETP* **60**, 953 (1984).
- [9] I. S. Berezin and N. P. Zhidkov, *Computing Methods*, 4th ed. (Pergamon Press, Oxford, 1965).
- [10] A. A. Samarskij and E. S. Nikolaev, *Numerical Method for Grid Equations* (Birkhauser, Basel, 1988), p. 284.
- [11] H. Choi and H. Takezoe, *Soft Matter* **12**, 481 (2016).